

Cooperative Spectrum Management in Cognitive Vehicular Ad Hoc Networks

Marco Di Felice*, Kaushik Roy Chowdhury[†], Luciano Bononi*

* Department of Computer Science, University of Bologna, Italy

Email: {difelice,bononi}@cs.unibo.it

[†] Department of Electrical and Computer Engineering, Northeastern University, Boston, USA

Email:krc@ece.neu.edu

Abstract—In recent years, Cognitive Radio (CR) technology has received significant attention from the research community as it enables on-demand spectrum utilization, based on the requests of the end-users. An interesting application area of CR technology is Vehicular Ad Hoc Networks (VANETs). In such networks, several innovative services and applications based on inter-vehicular communication have strict requirements in terms of bandwidth and delay, which might not be guaranteed by a fixed spectrum allocation paradigm. In this paper, we propose two key contributions pertaining to CR-VANETs: (i) an experimental study of the spectrum availability and sensing accuracy in a moving vehicle and (ii) a collaborative spectrum management framework (called Cog-V2V), which allows the vehicles to share spectrum information, and to detect spectrum opportunities in the licensed band. As part of this framework, we design a collaborative sensing and decision algorithm, enabling the vehicles to share spectrum information and to know in advance the spectrum availability at future locations along their motion paths. The simulation results, produced through a novel integrated simulation platform for CR networks, reveal significant improvements of Cog-V2V in sensing accuracy and pairwise communication performance compared to classical fixed spectrum approaches.

I. INTRODUCTION

Vehicular Ad Hoc Networks (VANETs) have attracted significant investment from industries and research institutions. In Europe, the potential benefits of cooperative vehicular communication systems are currently being explored in a number of research projects financed by the EU-FP7 [1], [2]. In these projects, a large variety of applications of VANETs have been identified and implemented, which include: adaptive cruise control systems, forward collision warning systems, fuel efficiency advisor systems, navigation systems, among others. In most cases, these technologies rely on existing wireless access standards for vehicular communication e.g. the WAVE and 802.11p [3], which utilize the 5.9 GHz spectrum band. Moreover, a new class of high bandwidth applications, such as public safety communication [23], traffic congestion detector [24], multimedia enabled driver assistance, car-to-car video streaming systems [25], among others, are being envisaged that can potentially saturate this band, leading to loss of the perceived quality or even complete failure for these applications.

As an example, the emerging spectrum scarcity problem (which impacts strict bandwidth-delay driven applications, such as public safety broadcast) in highly populated urban

areas in the 5.9GHz band in peak hours of traffic has been demonstrated by recent studies [10] [11]. At the same time, spectrum measurements reveal the presence of large tracts of vacant spectrum, i.e., portions of the UHF digital television (DTV) band, which are under-utilized in many urban areas [9]. Thus, solving the spectrum scarcity problem is a key issue in VANETs, and this is closely coupled with the need for providing an adequate Quality of Service (QoS) support for the emerging classes of high bandwidth and time-critical vehicular applications.

Cognitive Radio (CR) [4] is an enabling technology for improving the spectrum utilization of wireless systems. In a CR network, the CR nodes access the licensed spectrum in an opportunistic manner without causing any harmful interference to the licensed owners of the spectrum, also known as Primary Users (PUs) [4]. Although several applications of CR technology have been proposed in wireless mesh networks, emergency networks, health-care systems, among others, the potential of CR technology for VANETs (CR-VANETs) is far from being realized [12] [14]. For instance, CR-VANETs will enable mobile public safety operators to maintain essential communications in alternate bands in times of crises that impacted the regular communication channels [23]. The potential benefits of using CR technology for emergency networks, and in particular, the need for cooperation among vehicles in this context has been described earlier in [1].

In this paper, we address the following issues pertaining to CR-VANETs: (i) How might the constrained vehicular mobility affect the spectrum sensing activity performed by each vehicle? and (ii) How might the cooperation among vehicles improve the accuracy of sensing in an urban environment? To this aim, we use a methodological approach that involves devising algorithms for cooperative spectrum sensing in CR-VANETs, and the development of a new simulation platform with necessary software tools for a comprehensive performance analysis. These two main contributions in this paper are described below:

- We undertake spectrum measurements in a moving vehicle to determine the accuracy of spectrum sensing under different urban conditions and vehicular speeds. These experimental results confirm that the sensing accuracy is strongly affected by the channel characteristics unique

for the urban environment, which provides the basis and motivation for modeling of algorithms and protocols for CR-VANETs.

- We develop a cooperative spectrum management framework (called Cog-V2V) which allows each vehicle to collect spectrum sensing samples while moving, and to decide the spectrum availability at each location. This framework considers the impact of correlated-shadowing on the sensing output, and exploits the information coming from other vehicles.

We evaluate Cog-V2V performance through a new simulation platform which integrates (i) realistic modeling of the urban mobility with (ii) fine-grained characterization of wireless propagation in the urban environment, while incorporating the PU activity and CR-specific spectrum-aware functions.

The paper is organized as follows. In Section II, we review existing studies on CR-VANETs. In Section III we show the impact of the urban environment on the sensing activity performed by a moving vehicle through an experimental study. In Section V we describe our simulation platform, through which we implemented the Cog-V2V framework presented in Section IV. In Section VI, we evaluate the performance of the Cog-V2V framework under varying channel and network conditions. Conclusions follow in Section VII.

II. RELATED WORKS

Spectrum sensing constitutes an interesting and well-investigated research issue of CR networks [4]. However, to the best of our knowledge, the impact of mobility on spectrum sensing is yet to be well explored. In [8], the authors study the impact of mobility on the performance of spectrum sensing and corresponding tradeoffs between cooperation and scheduling. However, the mobility model in [8] can not be applied in CR-VANETs, where vehicles move along roads with fixed topologies. In [12] we discuss the unique role of vehicular mobility in the cooperation process, which might allow a vehicle to know in advance the spectrum availability on future locations along its path. An experimental analysis of the availability of TV channels for vehicles is proposed in [9], along a major interstate highway in the state of Massachusetts, USA. Some preliminary works demonstrate the benefits of cooperative sensing for CR-VANETs [10] [11] [12] [14]. In [10] [11] the authors propose a CR-based architecture in which data sensed by the vehicles are sent to road units that in turn forward the aggregated data to a processing unit. However, the centralized architecture is not suitable for supporting multi-hop communication on urban scenarios. In [14], the authors propose to apply Belief Propagation techniques to combine observations from different vehicles in a distributed manner, but they analyze the performance of the cooperative sensing scheme in a scenario with three vehicles only. To the best of our knowledge, [12] [14] are the only works addressing cooperative sensing over decentralized CR-VANETs. It can be shown that under hypothesis of conditional independence among sensing observations, the optimal fusion center is the *Likelihood Ratio Test* (LRT) [4]. However, the assumption of

independence among sensing observations does not hold in a CR-VANET, due to the correlation factor induced by the shadowing effect [5] [7]. As a result, we need to address decision techniques which must take into account the effect of correlation in a mobile environment, which is an important contribution in this paper.

III. EXPERIMENTAL ANALYSIS AND MOTIVATION

In this section, we show some preliminary results which demonstrate the impact of the urban topology and vehicular mobility on the performance of spectrum sensing performed by a CR vehicle. We conducted experiments at three locations, A, B and C, as shown in Figure 1(a) in the city of Boston, US. A universal software radio peripheral (USRP2) fixed on the roof of the car was used, running Gnuradio software [21] and the WBX daughterboard [22]. The USRP2 periodically scans the frequencies in the TV channels 21 – 51, and logs values into the host laptop. Owing to space constraints, we show readings only for channel 31, with a single PU transmitter active on that channel at location X of Figure 1(a). The individual measurement locations are approximately at the same straight line distance, and the propagation according to the online database TV Fool [20] is line of sight (LOS). We observe that in the downtown Boston area (first plot in Figure 1(b), location C in Figure 1(a)), the received power is subject to strong attenuation and fading. This is well contrasted with the measurements taken on the Harvard Bridge which has open space on either directions, and consequently, shows accurate signal detection (second plot in Figure 1(b), location B in Figure 1(a)). Finally, we vary speeds from 30 mph to 20 mph at location A, which is a straight street with moderately high structures on one side, and an open playing field on the other. Figure 1(b) (third and fourth plot) reveals that the signal strength lies mid-way between the above two cases, indicating a moderate fading environment. The spectrum sensing accuracy, expressed in terms of detection probability, is summarized in Table I. Here, we observe that the sensing accuracy decreases as the vehicle increases its average speed (Location A), in presence of moderate shadowing. While spectrum sensing accuracy is 100% in open spaces (Location B), the poor performance in high shadowing regions (Location C) highlights the need for an intelligent cooperation scheme. Especially in downtown urban areas, the slow moving traffic and the high shadowing conditions result in severe errors as most of the samples used by a single vehicle are correlated with previous ones, or from neighboring vehicles that are operating in the same region.

TABLE I
SPECTRUM SENSING ACCURACY

	Map Reference	P_d %
Location A:	Vassar St. (30 mph)	97.77
Location A:	Vassar St. (20 mph)	99.97
Location B:	Harvard Bridge (30 mph)	100
Location C:	High St (10 mph)	78.04

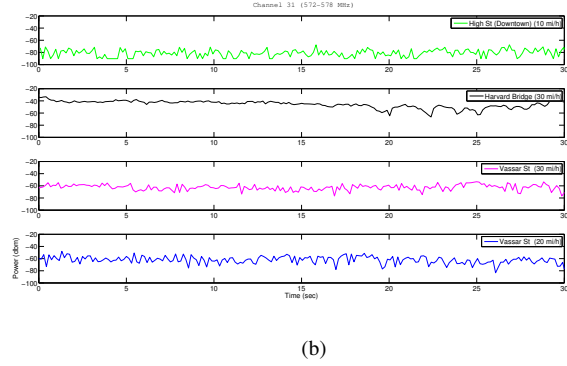
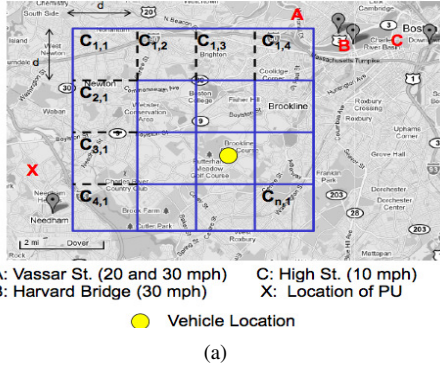


Fig. 1. The urban scenario (a) and received power measurement at three different locations A, B, C (b).

IV. THE COG-V2V FRAMEWORK

In this section, we explain the details of our CogV2V framework, beginning with an initial overview: Each vehicle on the street periodically senses the spectrum every T_s time units, on a set of M channels of the licensed band. The samples obtained during sensing are stored in a local *Spectrum Availability Database* (Section IV-A). From the locally measured information, each vehicle uses the two-hypotheses model [4] to decide between PU absence (H_0) or presence (H_1) on each channel, through a *correlation-aware decision* scheme (Section IV-C). After every T_b intervals, the content of the local database is broadcast on the Common Control Channel (CCC) (Section IV-D). Through the cooperation phase, vehicles can improve the accuracy of sensing on the current cell. Also, each vehicle can collect information about the availability of the licensed channels at future locations along their paths. Once a vehicle has detected the available spectrum opportunities on the current cell, the *spectrum allocation* scheme is responsible for deciding the channel to be used for communication between two vehicles, while the *spectrum sharing* scheme provides the functionalities for accessing the channel at MAC Layer. To ensure the practical relevance of our framework over existing technologies, we mainly rely on the IEEE 1609.4 standard, which allows the source-destination pair to coordinate transmissions in the Service Channel (SCH) slots [3]. For space shortage, we focus our attention on the cooperative spectrum sensing scheme, which is the main thrust of this work.

A. Spectrum Availability Database

In the Cog-V2V framework, each vehicle, e.g. vehicle ψ , keeps an updated view of the spectrum availability in a *Spectrum Availability Database* (SADB). The SADB contains the spectrum information (i) for the cell $C_{x,y}$ in which vehicle ψ is currently moving and (ii) for the set of adjacent cells that form the *spatial horizon* of vehicle ψ . The spatial horizon SH^ψ is defined in terms of number of cells as follows:

$$SH^\psi = \{C_{i,j} \text{ s.t. } \|x - i\| \leq h, \|y - j\| \leq h\} \quad (1)$$

where h bounds the number of adjacent cells in SH^ψ in the same row or column. For each cell $C_{i,j} \in SH^\psi$ and channel

f , we keep a Spectrum Availability Entry (SAE) which is structured as follows:

```
<SAE X Y Chan Available NumSamples Time >
... List of <SAMPLE> entries ...
</SAE >
```

Here, X, Y are the cell identifiers in the urban grid (i and j in this case), Chan is the channel id (f in this case), Available is a binary value which represents the availability of channel f in the cell $C_{i,j}$ (0=PU absent, 1=PU present), NumSamples is the number of sensing samples which determined the availability decision and Time is a time-stamp associated to the entry. Beside the aggregated spectrum availability information in a given cell, the SAE might also contain a list of <SAMPLE> entries which correspond to sensing samples produced by the vehicle ψ :

```
<SAMPLE Id Pos Speed Output Time Weight/>
```

Here, Id is a progressive number, Pos is the exact GPS-based position where sensing was performed, the speed of the vehicle ψ is contained in the Speed attribute, and the output of the sensing activity (Section IV-B) is saved in the Output attribute at a given instant Time. The Weight attribute is a measure of the relevance of the current <SAMPLE> on the decision process, and its meaning is clarified in Section IV-C. **Notation.** In the following, we denote with $SAE^\psi(C_{i,j}, f)$ the SAE entry in the SADB of vehicle ψ , for channel f and cell $C_{i,j}$. With the "." operator we access a specific field of a SAE. Analogously, we denote with Y_ψ^f the set of <SAMPLE> records for channel f and current cell $C_{x,y}$ and with s_i^f the i -th <SAMPLE> in Y^f .

B. Spectrum Sensing Operation

Every T_s time intervals, a vehicle ψ moving on cell $C_{x,y}$ performs sensing on a licensed channel f . We assume an energy-detector scheme is used at physical layer, i.e. the received power P_r^f on channel f is measured. Based on the threshold P_γ of the energy detector, the binary Output is calculated as follows:

$$\text{Output} = o_i^f = \begin{cases} 0 & \text{if } P_r^f \leq P_\gamma \\ 1 & \text{if } P_r^f > P_\gamma \end{cases} \quad (2)$$

Then, a new <SAMPLE> information is added to the $SAE^\psi(C_{x,y}, f)$. We realistically assume that a vehicle ψ can

sense only one channel among the available M at each T_s interval. Each vehicle ψ will sense the channel f with the lowest number of sensing samples in current SADB, i.e:

$$f = \operatorname{argmin}_c \{|Y^c|, 0 \leq c < M\} \quad (3)$$

It is important to highlight here that the spectrum horizon SH^ψ of vehicle ψ is dynamically changing over time as a consequences of the vehicle's mobility. For this reason, each vehicle ψ periodically removes the SAE entries which do not belong anymore to the spectrum horizon SH^ψ . Moreover, the entries in the SADB are removed after an expiration threshold.

C. Spectrum Sensing Decision

Every T_d time intervals, each vehicle analyzes the content of its SADB, and decides the availability of each channel in its current cell $C_{x,y}$ through a soft decision scheme. Several merging rules for cooperative sensing have been proposed in the literature [4]–[6]. However, classical merging schemes based on OR, AND or voting rules assume the independence among samples, and thus might result in suboptimal performance in the presence of correlated shadowing [4]. At the same time, most of the correlation-aware cooperative sensing schemes proposed so far find limited application in CR-VANETs for these reasons: (i) they are based on computationally expensive statistical techniques, which can not be used for on-line PU detection on off-the-shelf mobile devices [5], [6], (ii) they introduce an high network overhead for the convergence of the decision algorithms [14]. For these reasons, we propose here a novel decision algorithm, which takes into account the effect of correlation on aggregating the samples, but at same time it is easy to be implemented on mobile devices with limited processing and communication capabilities. This makes our approach suitable for use in CR-VANETs. In our approach, given a set of observations Y^f stored for a given channel f in the SADB, each sample s_i^f ($i \in Y^f$) is assigned a different Weight w_i^f . We find the overall decision by considering the Output o_i^f of each sample and its weight w_i^f . The overall cooperative decision D between H_0 and H_1 is based on the weighted-majority of the samples:

$$D^f = \begin{cases} H_0 & \text{if } \sum_{i \in Y^f} w_i^f \cdot o_i^f \leq \kappa \\ H_1 & \text{if } \sum_{i \in Y^f} w_i^f \cdot o_i^f > \kappa \end{cases} \quad (4)$$

where κ is a threshold on detection (set to 0.5 in our experiments). As the success of the proposed detection relies strongly on the judicious choice of w_i^f , Algorithm 1 assigns and modifies these weights with time.

First, we define the correlation function between two samples s_i and s_j based on the model proposed in [18]:

$$R(s_i, s_j) = e^{-\frac{d}{d_{corr}} \cdot \ln 2} \quad (5)$$

where d is the distance between the samples and d_{corr} is the decorrelation function set to 20 m for the urban environments. Then, we provide the main steps of the decision algorithm:

- 1) *Step1. Initial Weight Assignment:* Initially, the weight of a sample s_i^f is set as:

$$w_i^f = 1 - \frac{\sum_{s_j^f \in Y^f} R(s_i^f, s_j^f)}{\sum_{s_k^f \in Y^f} \sum_{s_j^f \in Y^f} R(s_k^f, s_j^f)} \quad (6)$$

where $R(\cdot, \cdot)$ is the distance dependent correlation index defined by equation 5. Intuitively, samples corresponding to isolated positions get higher weights because less correlated with the other samples. However, simply picking the samples based on their initial weights might not result in a good coverage of the environment, as shown in Figure 2(a). Consider Figure 2(a) showing samples $s_1 \dots, s_9$ collected over different increasing distances on the horizontal plane¹. The sample numbers and the respective initial weights are shown in the table. Sample s_1 is first chosen, and by the simple ordering of initial weights, sample s_2 would be picked next (second highest weight). However, both s_1 and s_2 are present in the same shadow region of the tall buildings, and hence, an error in one of them is likely to be present in the other. This selection may strongly bias the overall decision D erroneously.

- 2) *Step2. Iterative Weight Adjustment:* Once the sample s_k^f with the highest weight is chosen, it is removed from the set Y^f . Then, we reduce the weights of all other remaining samples in Y^f based on their correlation (in terms of distance) with sample s_k^f . In Figure 2(b), we show the weight assignment after the first iteration of the algorithm. It can be noticed that since sample s_1 was chosen earlier, the weight of sample s_2 is greatly reduced. Similarly, the next highest weight sample is identified and then removed from Y^f , with the other sample weights adjusted with respect to its own. These iterations continue till, one by one, all the samples are accounted for and $Y^f = \{\}$.
- 3) *Step3. Weight Normalization:* We normalize the weights of all the samples as the end of Step 2. by dividing by the sum of the weights, so that $\sum_{i \in Y^f} w_i^f = 1$. This ensures the individual weights $w_i^f \in [0, 1]$. The final weight assignment is shown in Figure 2(c). Due to space constraints we omit the proof for the fairly straightforward derivation of the computation complexity of this algorithm, which is found to be $O(n^2)$.
- 4) *Step4. Cooperative Sensing Decision:* The cooperative decision is then made for all the M channels in the licensed band using (4), so that each vehicle can build a set of available channels where the weighted decision $D = H_0$.

D. Spectrum Information Sharing

Every T_b time intervals, each vehicle ψ broadcasts spectrum information on the Common Control Channel (CCC)²

¹The superscript f is dropped in the figures for ease of disposition.

²We assume that broadcast information are sent on the CCC during the Control CHannel (CCH) slots foreseen by the IEEE 1609.4 scheme [3].

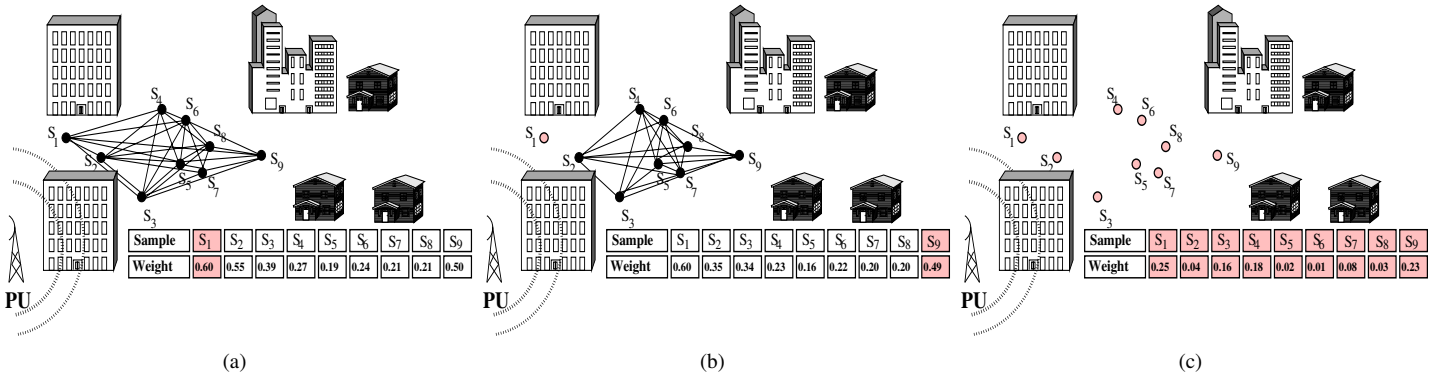


Fig. 2. Example scenario for the Sensing Decision algorithm: Figure 2(a) shows the initial weight assignment, Figure 2(b) shows the weight configuration after the first iteration in which sample s_1 is chosen and removed from the set Y^f , Figure 2(c) shows the final weight assignment of the algorithm.

Algorithm 1 Sensing Decision Algorithm

```

1 Initial Weight Assignment
for each sample  $s_i \in Y^f$  do
     $w_i^f = 1 - \frac{\sum_{s_j^f \in Y^f} R(s_i^f, s_j^f)}{\sum_{s_k^f \in Y^f} \sum_{s_j^f \in Y^f} R(s_k^f, s_j^f)}$ 
end for
 $R_{max} = \max \{R(s_i^f, s_j^f) \forall s_i^f, s_j^f \in Y^f\}$ 
2 Iterative Weight Adjustment
repeat
    choose  $s_k^f = \text{argmax } w_i^f \forall s_i^f \in Y^f$ 
     $Y^f = Y^f - \{s_k^f\}$ 
    for each sample  $s_j^f \in Y^f$  do
         $w_j^f = w_j^f \cdot (1 - \frac{R(s_k^f, s_j^f)}{R_{max}})$ 
    end for
until  $Y^f = \emptyset$ 
3. Weight Normalization
 $w_{sum} = \sum_{s_i^f \in Y^f} w_i^f$ 
for each sample  $s_j^f \in Y^f$  do
     $w_j^f = \frac{w_j^f}{w_{sum}}$ 
end for
4. Cooperative Sensing Decision
 $D = \sum_{s_i^f \in Y^f} w_i^f \cdot o_i^f$ 
if  $D < \gamma$  then
    Decide for  $H_0$  on channel  $f$  (PU absent)
else
    Decide for  $H_1$  on channel  $f$  (PU present)
end if

```

through a SENSE message. Since fitting the full content of the SADB in each SENSE message might introduce a significant network overhead, we utilize a more conservative approach in which vehicle ψ broadcasts: (i) the complete SAE entry for the current cell $C_{x,y}$, including a subset of <SAMPLE> records for each channel f and (ii) the SAE with only the aggregated spectrum information for each cell $C_{i,j} \in SH^\psi$ (i.e. the Available, NumSamples and Time fields) and channel f . On receiving a SENSE message from vehicle ψ , vehicle η (i) adds the <SAMPLE> records to its SADB and (ii) updates the SAE entry for the cells belonging to its spectrum horizon SH^η . To this aim, it is reasonable to assume

that a vehicle collecting more sensing samples on a given channel/segment can provide higher accuracy on PU detection. Based on such considerations, we design a probabilistic update rule where vehicle η will replace the aggregated information of its $SAE^\eta(C_{i,j}, f)$ with $SAE^\psi(C_{i,j}, f)$ with a probability P_u given by:

$$P_u = \max \left\{ \alpha \left(1 - \frac{n_f^\eta}{n_f^\psi} \right), 0 \right\} \quad (7)$$

where $n_f^\psi = SAE^\psi(C_{i,j}, f).NumSample$, n_f^η is the number of samples which determined the spectrum decision on channel f for vehicle η and $0 \leq \alpha \leq 1$ is a factor regulating the amount of cooperation among vehicles (set to 0.7 in our experiments). Algorithm 2 shows the steps performed by vehicle η after the reception of a SENSE message from vehicle ψ .

Algorithm 2 SADB Update Algorithm

```

Vehicle  $\eta$  receives a SENSE message from node  $\psi$ 
for each  $SAE^\psi(C_{i,j}, f)$  contained in the SENSE message do
    if  $C_{i,j} \in SH^\eta$  then
        Add <SAMPLE> records (if any) to the  $SAE^\eta(C_{i,j}, f)$ 
         $n^\psi = SAE^\psi(C_{i,j}, f).NumSamples$ 
         $n^\eta = \max\{|Y_f^\eta|, SAE^\eta(C_{i,j}, f).NumSamples\}$ 
        Compute  $P_u = \max \left\{ \alpha \left( 1 - \frac{n_f^\eta}{n_f^\psi} \right), 0 \right\}$ 
        if  $P_u > \text{Random}[0:1]$  then
             $SAE^\eta(C_{i,j}, f).Available = SAE^\psi(C_{i,j}, f).Available$ 
             $SAE^\eta(C_{i,j}, f).NumSamples = SAE^\psi(C_{i,j}, f).NumSamples$ 
        end if
    end if
end for

```

V. SIMULATION PLATFORM

We evaluate the performance of Cog-V2V through an integrated simulation platform (shown in Figure 3) that takes into account the topology and structural features from an open-source mapping software, and combines these with a physical channel model. The constituent blocks and their interactions are explained as follows:

- **Mobility Trace Generator:** We generated the mobility trace of the vehicles through the SUMO tool [19], which is

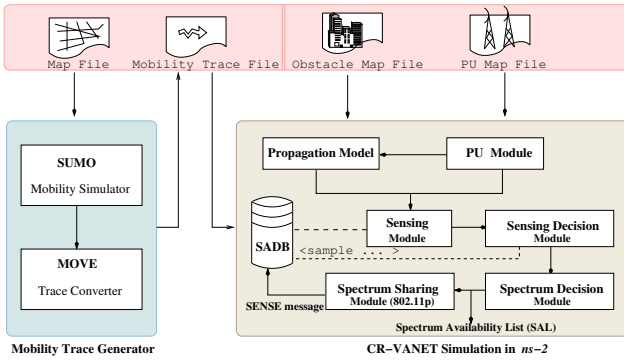


Fig. 3. The CR-VANETs integrated simulation environment.

an open-source microscopic traffic road simulation package designed to handle large road networks. As output, the SUMO tool produces a mobility trace file which can be imported into the *ns-2* tool. The generated urban scenario is divided into grids, in which each cell $C_{i,j}$ is a square with side length equal to d , and is uniquely identified by horizontal and vertical indices i, j (Figure 1(a)). The cell boundaries are made known to all the vehicles.

• **CR-VANETs Simulation in *ns-2*:** We considerably extended the *ns-2* tool implementing the models of: (i) wireless signal propagation and path loss in presence of obstacles (i.e. the *Propagation Module*), (ii) PU activity over time (i.e. the *PU Module*), (iii) CR cycle functionalities including: *Spectrum Sensing*, *Spectrum Decision*, and *Spectrum Sharing*. The PU map file contains the description of PU characteristics and activity in the current scenario, i.e., the PU location coordinates, transmitting power, active channel, and its ON/OFF activity over time as modeled in [15]. Analogously, the obstacle map file contains the location of obstacles and buildings located on the side of the streets that cause *shadowing* or *large-scale fading*. More specifically, each obstacle of the scenario is described by a corresponding `<obs>` entry in the obstacle map file:

$$\langle \text{obs } N \ x_1 \ y_1 \ \dots \ x_N \ y_N \ h \ \beta \ \gamma \ l \rangle$$

where N is the number of vertices composing the polygon (polygonal shape of the building is assumed), x_i, y_i are the 2-D coordinates of the i -th vertex, h is the obstacle height, β_i is the attenuation caused by the exterior walls (dB) and γ_i is the attenuation caused by the internal structure (dB/m). Based on the obstacle map file and on the PU map file, the *Propagation Model* computes the power received $P_r(\text{dBm})$ at generic positions of the urban map as in [17]:

$$P_r(\text{dBm}) = P_t(\text{dBm}) + G_t(\text{dB}) + G_r(\text{dB}) - \sum L_x(\text{dB}) \quad (8)$$

Here, P_t is the PU transmit power, G_t and G_r are the antenna gains and L_x represents the large-scale path loss, modelled through the summation of three terms:

$$L_x(\text{dB}) = L_{att}(\text{dBm}) + L_{sha}(\text{dB}) + L_{obs}(\text{dB}) \quad (9)$$

The L_{att} term is the attenuation caused by the source-receiver distance (without noise), and is derived through a classical two-ray ground propagation model [16]. The L_{sha} term is the path loss caused by shadowing effect, and is derived through a log-normal shadowing model [16]. The L_{obs} term is the signal attenuation caused by the presence of obstacles in the urban environment, as proposed in [17]:

$$L_{obs}(\text{dB}) = \sum_{j=0}^P (\beta_j \cdot n_j + \gamma_j \cdot d_j) \quad (10)$$

where P is the total number of intersecting obstacles on the LOS, n_j is the number of intersections between the LOS and the j -th obstacle, d_j is the total length of such intersections, and β_j and γ_j are the obstacles' attenuation characteristics described before. Then, we model the CR-cycle functionalities of each vehicle through the *Spectrum Sensing*, *Spectrum Decision* and *Spectrum Sharing* modules. For space shortage, we omit further details of the CR models, which are described also in [13].

VI. PERFORMANCE EVALUATION

In this section, we discuss the performance of Cog-V2V. In Section VI-A we provide the model parameters and metrics, and in Section VI-B we show the performance results.

A. Simulation Parameters

Through the integrated tool described in Section V, we evaluated the Cog-V2V framework for different urban scenarios and network configurations. We considered a street portion of 1 km length, divided into cells of $d = 100$ m length. The vehicles move on two lanes (one for each direction) with speed $v < 15$ m/s. The licensed spectrum band is divided into $M = 5$ channels, and each channel can be occupied by a TV broadcast PU, which is always active. Each PU transmits with a power of 27 dBm. PUs are located at the borders of the cells, so that: (i) the activity of a single PU can affect multiple cells of the street and (ii) there is at least one spectrum hole available for vehicles in each cell. We place six clusters of buildings at the side of the street. We vary the traffic intensity on the street, the attenuation factor caused by the inner structure of the obstacles (i.e. the γ factor of equation 10), and the spectrum sensing interval T_s .

We evaluate the performance of the Cog-V2V framework through the following metrics:

- *Probability of detection (P_d)*. This is defined as the probability that a vehicle detects the presence of a PU on the current channel, at each decision interval (T_d). Conversely $1 - P_d$ is the probability that the sensing decision algorithm mis-detects the presence of a PU on the current channel.
- *Spatial Vulnerability Index (SVI)*. In case of PU mis-detection on the current channel and cell, this is defined as the fractional of the cell length after which a vehicle detects the PU presence on the current channel. More

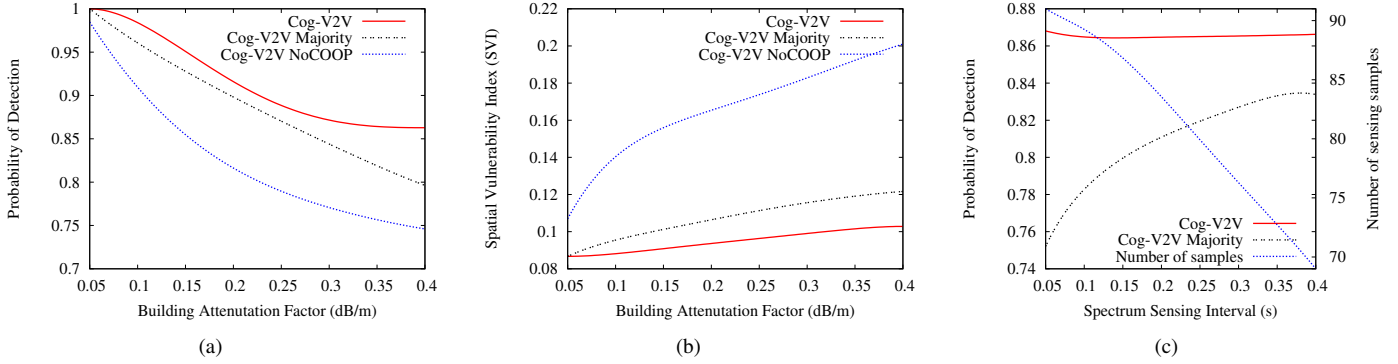


Fig. 4. Figure 4(a) and 4(b) show the P_d and the SVI metrics as a function of γ . The P_d metric over T_s is shown in Figure 4(c).

specifically, the SVI metric is defined as in [12]:

$$SVI = \min \left\{ \frac{\text{space_covered}}{d}, 1 \right\} \quad (11)$$

where d is the cell length, and space_covered is the distance covered by the vehicle from the starting boundary of the cell till the location where the PU was detected. If the vehicle traverses completely through the cell without detecting the PU activity, then we normalize SVI to 1. This metric gives the responsiveness of the system.

B. Simulation Results

In Figures 4(a) and 4(b) we show the performance of the Cog-V2V framework when we vary the amount of attenuation factor for non-LOS locations, given by the γ factor of Equation 10 (we assume β is fixed and equal to 2dB as in [17]). Through the varying γ , we model different propagation characteristics of the obstacles inbetween the PU and the vehicles. We evaluate three different configurations of Cog-V2V:

- *Cog-V2V*: we consider the full configuration of our framework, with both the cooperation scheme (Section IV-D) and the correlation-aware decision scheme (Section IV-C) enabled.
- *Cog-V2V Majority*: the cooperation scheme (Section IV-D) is enabled, but not the correlation-aware decision scheme (Section IV-C). Each vehicle decides between the H_0 and the H_1 hypotheses by applying the MAJORITY rules [4] to local and received samples.
- *Cog-V2V NoCOOP*: the cooperation scheme (Section IV-D) is disabled. Each vehicle decides between the H_0 and the H_1 hypotheses by applying the correlation-aware decision scheme (Section IV-C) to the samples collected by the vehicle itself on the current cell.

We consider a traffic intensity of 0.5 vehicle/s, i.e. a new vehicle enters the street every 2s. Figure 4(a) shows the P_d index over the attenuation factor γ . Both the *Cog-V2V* and *Cog-V2V Majority* frameworks use a frequency of broadcast (T_b) equal to 1s. For small values of γ , all the configurations provide error-free detection of the PU signal. However, the accuracy of the *Cog-V2V NoCOOP* decreases when we increase the amount of attenuation caused by buildings. The accuracy

of the *Cog-V2V Majority* framework decreases to 80% for $\gamma = 0.4$ dB/m, due to the correlation among the available samples. In *Cog-V2V*, we assign different weights to each sample, based on its spatial diversity. As a result, *Cog-V2V* can provide robust PU detection also under high shadowing conditions. In Figure 4(b) we show the SVI index as a function of the attenuation factor γ . If a vehicle relies on individual sensing only (e.g. in the *Cog-V2V NoCOOP* configuration), it will detect the presence of a PU on the current channel only after having covered almost 20% of the current cell length d (which is 100m in our experiments). In *Cog-V2V* with $T_b = 1$ s, the SVI index decreases to less than 0.9% due to the fact that a vehicle ψ can receive information from the other vehicles. Thus, a vehicle can be informed about the presence of a PU on future locations of the path before accessing them. In Figure 4(c), we show the P_d index of the *Cog-V2V* and *Cog-V2V Majority* frameworks when we vary the spectrum sensing interval (T_s) on the x -axis. We consider a configuration with $\gamma = 0.4$ dB/m. In the same Figure, we also depict (on the $x - y$ axes) the average number of sensing samples collected by each vehicle on the current cell. As expected, increasing the sensing interval (T_s) produces a reduction of the number of sample available to each vehicle (the blue line on the $x - y$ axes), while extending the transmission opportunities for the CR vehicles. However, Figure 4(c) shows that the performance of *Cog-V2V* are slightly affected by the sensing interval. This is due to the fact that the decision algorithm of Section IV-C utilizes only a subset of the available samples in presence of high spatial correlation of the data. As a result, *Cog-V2V* can improve the spectrum exploitation by reducing the sensing frequency performed by vehicles without increasing the interference caused to the PUs. At the same time, Figure 4(c) shows that the P_d index of *Cog-V2V Majority* improves by increasing the sensing interval. These results confirm the analysis in [8].

In Figures 5(a) and 5(b), we show the performance of the three framework configurations as a function of the vehicle intensity. We consider this scenario: $T_b = 1$ s, $T_s = 0.2$ s and $\gamma = 0.4$ dB/m. The performance of *Cog-V2V NoCOOP* are not affected by the vehicle intensity. Conversely, *Cog-V2V* and *Cog-V2V Majority* work better under moderate and high traffic

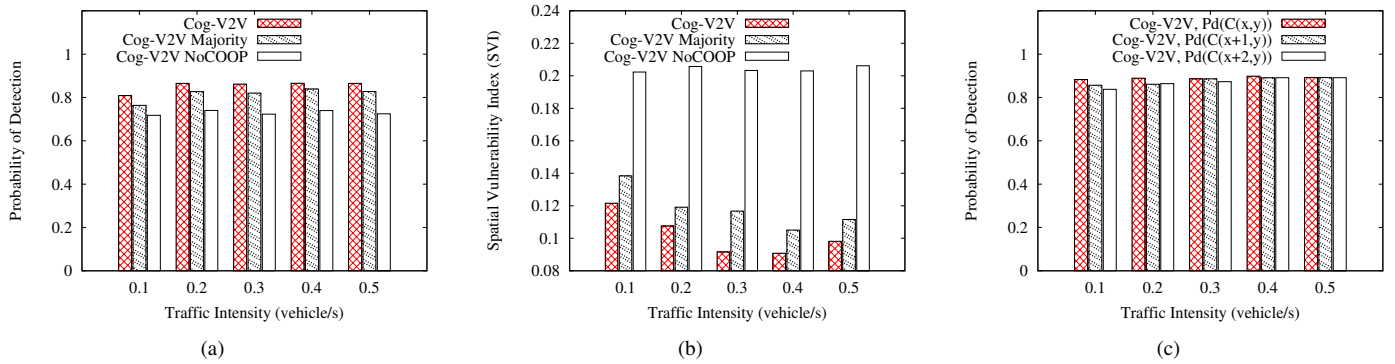


Fig. 5. Figure 5(a) and 5(b) show the P_d and the SVI metrics as a function of the traffic intensity. $P_d(C_{x+h,y})$ is shown in Figure 5(c).

conditions, because each vehicle can collect more samples from its neighbours. At the same time, Figure 5(a) shows that the performance of cooperative schemes become stable or slightly decreases under high traffic conditions, due to the MAC collisions on broadcast messages. The improvement provided by *Cog-V2V* in terms of the SVI index can be seen in Figure 5(b). In Figure 5(c) we test the ability of *Cog-V2V* to perform accurate allocation in advance in the spectrum horizon SH . In our experiment, each vehicle performs sensing decision on the current cell $C_{x,y}$, and on cells at distance one ($C_{x+1,y}$) and two ($C_{x+2,y}$). Figure 5(c) shows $P_d(C_{x+h,y})$, with $h=0,1,2$, as a function of the traffic intensity. The results in Figure 5(c) demonstrate that the allocation accuracy depends on the cell distance and on the amount of spectrum information available at each node. In case of low traffic density, the accuracy of the allocation decreases when predicting the spectrum conditions over more than one segment of distance. For vehicle densities higher than 0.4 vehicles/s, the allocation over next two cells ($P_d(C_{x+2,y})$) is as accurate as the allocation over the current cell ($P_d(C_{x,y})$).

VII. CONCLUSIONS

This paper presented *Cog-V2V*, a complete framework for spectrum sensing, decision and sharing in CR-VANETs. We have undertaken real world experiments to determine the need for a novel cooperative correlation-based approach for spectrum sensing in mobile vehicular environments. Through a novel simulation platform for CR-VANETs, we have evaluated the performance of *Cog-V2V* in several urban scenarios, and we have shown that our correlation-based cooperative sensing can provide robust and accurate PU detection under high shadowing conditions. Our future research directions include: studying the impact of vehicular speeds and Doppler-shift induced effects on the sensing performance and implementing the *Cog-V2V* framework on USRP2 devices.

REFERENCES

- [1] Cooperative Vehicle-Infrastructure Systems, (CVIS) EU FP-7 Project. Website [Online]: <http://cvisproject.org>
- [2] PRE-DRIVEC2X EU project. <http://www.pre-drive-c2x.eu>. FP7.
- [3] "Wireless LAN Medium Access Control (MAC) and Physical Layer (PHY) Specifications: Wireless Access in Vehicular Environment *IEEE Std 802.11p/D7.0*, 2009.
- [4] I. F. Akyildiz, B. F. Lo, and R. Balakrishnan. Cooperative Spectrum Sensing in Cognitive Radio Networks: A Survey. *Physical Communication* (Elsevier), 4(1), pp. 4062, 2011.
- [5] B. Kasiri and J. Cai. Effects of correlated shadowing on soft decision fusion in cooperative spectrum sensing. in Proc. of ACM CWCN, 2010.
- [6] I. Unnikrishnan and V. Veeravalli. Cooperative Spectrum Sensing and Detection for Cognitive Radio. in Proc. of IEEE GLOBECOM, 2007.
- [7] T. Do and B. L. Mark. Joint spatial-temporal spectrum sensing for cognitive radio networks. *IEEE TVT*, 59(7), pp. 3480-3490, 2010.
- [8] A.W. Min and K.G. Shin. Impact of Mobility on Spectrum Sensing in Cognitive Radio Networks. in Proc. of ACM CORONET, 2009.
- [9] S. Pagadarai, A. M. Wyglinski and R. Vuyyuru. Characterization of Vacant UHF TV Channels for Vehicular Dynamic Spectrum Access. In Proc. of IEEE VNC, 2009.
- [10] X. Y. Wang and P.-H. Ho. A Novel Sensing Coordination Framework for CR-VANETS. *IEEE Transactions on Vehicular Technology*, 59(4), pp. 1936-1948, 2010.
- [11] K. Fawaz, A. Ghandour, M. Olleik and H. Artail. Improving Reliability of Safety Applications in Vehicle Ad hoc Networks through the Implementation of a Cognitive Network. in Proc. of IEEE ITC, 2010.
- [12] M. Di Felice, K.R.Chowdhury and L.Bononi. Analyzing the potential of Cooperative Cognitive Radio Technology on inter-vehicle communication. in Proc. of IFIP Wireless Days, 2010.
- [13] M. Di Felice, K.R.Chowdhury, W. Kim, A. Kassler and L.Bononi. End-to-end protocols for Cognitive Radio Networks: An Evaluation Study. *Performance Evaluation* (Elsevier), 68(9), pp. 859-875, 2011.
- [14] H. Li and D. Irick. Collaborative Spectrum Sensing in Cognitive Radio Vehicular Ad hoc Networks: Belief Propagation on Highway. in Proc. of IEEE VTC Spring, 2010.
- [15] W. Y. Lee and I. Akyildiz. Optimal Spectrum Sensing Framework for Cognitive Radio Networks. *IEEE Transactions on Wireless Communication*, 7(10), pp. 3845-3857, 2008.
- [16] T. S. Rappaport. *Wireless communications: Principles and Practice*. Prentice Hall Press, 2002.
- [17] C. Sommer, D. Eckhoff, R. German and F. Dressler. A Computationally Inexpensive Empirical Model of IEEE 802.11p Radio Shadowing in Urban Environments. University of Erlangen, Technical Report, 2010.
- [18] M. Gudmundson. Correlation Model for Shadow Fading in Mobile Radio Systems. *IEEE Electronics Letters*, 27(30), pp. 2145-2146, 1991.
- [19] Simulation of Urban MObility (SUMO) Project. Website: <http://sumo.sourceforge.net>.
- [20] TV Fool Coverage Maps. Website [Online]: <http://www.tvfool.com/>
- [21] GNU Radio Project. Website [Online]: <http://www.gnuradio.org>
- [22] Ettus Research LLC, USRP Family Datasheet. Website [Online]: <http://www.ettus.com/>
- [23] The 9/11 Commission Report. Final report of the national commission on terrorist attacks upon the United States. Website [Online]: <http://www.gpoaccess.gov/911/pdf/fullreport.pdf>
- [24] G. Marfia and M. Roccetti. Vehicular Congestion Detection and Short-Term Forecasting: A New Model with Results. *IEEE Transactions on Vehicular Technology*, 60(7), pp. 2936-2948, 2011.
- [25] T. Hossain, Y. Cui and Y. Xue. Vanets: Case Study of a Peer-to-Peer Video Conferencing System. in Proc. of IEEE CCNC, 2009.